Biochimica et Biophysica Acta 933 (1988) 276–287
Elsevier

BBA 42749

Theoretical and experimental study of trapping times and antenna organization in pea chloroplasts by means of the artificial fluorescence quencher *m*-dinitrobenzene

C. Kischkoweit, W. Leibl and H.-W. Trissl

Schwerpunkt Biophysik, Universität Osnabrück, Osnabrück (F.R.G.)

(Received 25 August 1987)
(Revised manuscript received 9 December 1987)

Key words: Fluorescence induction; Light gradient photovoltage; Reaction center; Photosystem I; Photosystem II; Alpha center; Beta center

The quenching effect of *m*-dinitrobenzene on the fluorescence under F_{max} and F_0 conditions as well as on the light-gradient photovoltage, V, from pea chloroplasts with stacked thylakoids has been examined theoretically and experimentally with respect to trapping times and antenna organizations (lake or separate unit model). The rationale for these experiments was that the fluorescence is a probe for Photosystem II, whereas the photovoltage is a probe for Photosystem I (Trissl, H.-W., Breton, J., Deprez, J. and Leibl, W. (1987) Biochim. Biophys. Acta 893, 305–319). In Stern-Volmer plots, all three quantities (F_{max}, F_0, V) could be described by straight lines with different slopes. Equations were derived which show that the ratio of these slopes relates in a simple way the fluorescence decay time at F_{max} with the trapping times. With this method we determined the trapping time in Photosystem I to be 97 ± 10 ps. Furthermore, we have derived a unified formalism for different photosystems having either different or alike antenna organizations. This theory permits us to relate in a consistent way the present data to several other data reported in the literature. However, it does not allow us to elucidate the organization of the PS I antenna, since the theoretically expected difference between the lake and separate unit models was smaller than the experimental accuracy.

Introduction

The absolutely primary processes in photosynthesis are the absorption of photons by so-called antenna pigments, the energy migration within the antenna system, and finally the trapping and photochemical conversion by the reaction centers. The absorption process creates an excited singlet state that, in the general case, is subject of various competing deactivation processes, like radiationless internal conversion, intersystem crossing to triplet states, fluorescence and photochemistry, i.e., trapping (for review see Refs. 1–3). A high quantum yield of photosynthesis requires that the photochemical path is the main decay route. Consequently the fluorescence decay kinetics which probes the concentration of the excited states in the antenna system can be used for monitoring the trapping kinetics. This is a

Abbreviations: DCMU, 3-(3-,4-dichlorophenyl)-1,1-dimethylurea; DMSO, dimethyl sulfoxide; DNB, *m*-dinitrobenzene; PS I, Photosystem I of green plants; PS II, Photosystem II of green plants; Q_A, first quinone acceptor of Photosystem II; RC, reaction center.

Correspondence: H.-W. Trissl, Schwerpunkt Biophysik, Universität Osnabrück, Barbarastrasse 11, D-4500 Osnabrück, F.R.G.

current way to measure trapping kinetics.

In chloroplasts from higher plants, containing two types of photosystem (PS I and PS II), the fluorescence originates mainly from PS II [4]. With open RCs the PS II fluorescence intensity is termed F_0. Photosystem I is only weakly fluorescent [5–7]. Therefore, in experiments with slowly incoming photons (continuous light) the PS I fluorescence does not significantly interfere with the PS II fluorescence. The yield of the PS II fluorescence increases in a sigmoidal way to a maximal level, F_{max}, as the concentration of the reduced first quinone acceptor, Q_A, increases (presence of the inhibitor, DCMU) [8]. Detailed kinetic analysis of these fluorescence induction curves has demonstrated a heterogeneity of PS II, the α- and β-centers (PS II_α and PS II_β) [9–11]. They differ in various molecular properties [12]. For instance, α-centers have a larger antenna size than β-centers [10,13,14].

Another difference between α- and β-centers is evident in fluorescence decay analysis by the single photon timing technique [15]. If the fluorescence decay in pea or spinach chloroplasts is analyzed with four exponentials, α- and β-centers can be distinguished by their kinetics. PS II_α appears with a 190–270 ps component and PS II_β with a 500–600 ps component [7,12]. Photosystem I is contributing to the fluorescence with a 70–100 ps phase. Closure of PS II_α leads to a 1.9 ns phase and closure of PS II_β to a 0.62 ns phase [7].

According to the heterogeneous photosystems (PS I, PS II_α, PS II_β, and eventually unconnected antenna pigments), fluorescence decay measurements require sophisticated analysis that may involve up to eight fit parameters (amplitudes and time constants of four components) [15]. Handicaps for the determination of the trapping time in PS I by the fluorescence method are the small quantum yield and the fast decay, which is near the instrumental time resolution. The reported values range from 40 ps to 110 ps [16,17]. Particularly when all RCs are open, there are three kinetic phases which are rather close together and may mix. However, when PS II is closed the kinetic phases are more separated [7] (see also Table I).

A method different from fluorescence for determination of trapping times recently became available in the form of the time-resolved photoelectric 'light-gradient' method [18–20]. This method is based on a direct electrical detection of the arrival and photochemical conversion of excitons at the RC. The trapping time in PS I determined by this method was reported to be 90 ± 20 ps [21].

As will be shown in this study, a further way to evaluate trapping times without the need of extremely high time resolution is the use of an artificial quencher, like DNB, which combines the measurement of fluorescence induction and photovoltage. In addition, artificial quenchers may give information on the organization of antenna systems.

An artificial quencher opens an additional competing deactivation path for the singlet exciton, thereby decreasing the yields of all other decay paths, especially those of fluorescence and trapping [22–24]. In the simplest model of a homogeneous system, the decreased yields of the deactivation quantities can be described by the Stern-Volmer equation, which predicts a linear dependence of the reciprocal yield on the concentration of the quenching substance. Such linear behavior has been found for the fluorescence at the F_o and F_{max} levels in the alga *Chlorella vulgaris* and the cyanobacterium *Cyanidium caldarium* [24].

For PS II, ample evidence exists in favor of an antenna system belonging to the matrix type, where the excitation energy can freely migrate from one unit to another. The evidence comes mostly from fluorescence yield measurements when the system is progressively moved from 100% open to 100% closed RCs (fluorescence induction curves) [2,3]. The situation is less clear for PS I, whether or not it belongs to the 'separate units' type, where the excitation energy is restricted to a particular photosynthetic unit [2,25,26]. The question was addressed recently by absorption spectroscopy [25] and photovoltage measurements [21]. Here we attempt to answer the question by means of the artificial quencher, DNB [27].

This artificial quencher has already been used to investigate antenna organizations [24]. It was shown by a theoretical treatment that straight lines in the Stern-Volmer plots are characteristic for the matrix model and curves with positive curvature for separate units. From the experimental finding of straight lines, the matrix model for

PS II was concluded [24]. However, the degree of curvature depends strongly on the statistical distribution of the quencher molecules and the assumed rate constant for quenching. Therefore, in practice, the possibility to discriminate between the two models rests on the assessment of the actual partition coefficient of the quencher between the water and the membrane phase and on the actual quenching rate constant.

In the present study we extend the formalism derived by Sonneveld et al. [24] by (i) including the α-,β-heterogeneity of PS II and (ii) introducing a common fit parameter for the matrix and separate unit model. This parameter is then used to fit Stern-Volmer plots of fluorescence (i.e., PS II) and photovoltage (i.e., PS I). Furthermore, we measure the partition coefficient of DNB and use it to calculate the quenching rate constant of a chlorophyll-DNB collision complex. The numerical values then give a criterion for the feasibility to distinguish by the 'artificial quencher' method between a matrix and a separate unit model in the case of PS I.

Materials and Methods

Stacked chloroplasts of 12–16-day-old pea seedlings (*Pisum sativum*) were prepared as described [28]. Mitochondria and other cell organelles are discarded with the supernatant at the first centrifugation step at $1000 \times g$. The envelope membranes were disrupted by an osmotic shock and the major part of them remained in the supernatant of the second centrifugation at $10000 \times g$. All media contained 5 mM $MgCl_2$. The chloroplasts were stored until use at liquid nitrogen temperature in a medium containing 30% ethylene glycol. For all measurements this stock solution was adjusted to 3.5 mM chlorophyll by diluting it with 100 mM Sorbitol, 10 mM Tricine (pH 7.8), 10 mM NaCl and 5 mM $MgCl_2$.

m-Dinitrobenzene was dissolved in DMSO as stock solutions at appropriate concentrations (including zero) so that the final DMSO concentration in the chloroplast suspension was 2% at any DNB concentration. DCMU was dissolved in DMSO at a concentration of 10 mM and added to the chloroplasts to give a final concentration of 100 μM ([DCMU]/[Chl] = 0.029). This resulted in an additional DMSO concentration of 1%. DCMU was always added before DNB. Control experiments showed that 4% DMSO alone had no effect on either the fluorescence induction curves or the photovoltage.

The photoelectric measurements of the light-gradient type were carried out in a capacitative microcoaxial cell as described [21]. The optical path was 0.1 mm. The photovoltage was picked-up by a 500 MHz impedance converter, amplified, and recorded on a 1 GHz oscilloscope equipped with a digitizing camera.

The flash excitation occurred with a Q-switched and frequency-doubled Nd-YAG laser which delivered pulses of 12 ns duration. Homogeneous illumination of the sample was achieved by a bifurcated light pipe with the common end placed 7 cm above the measuring cell.

The fluorescence induction curves were performed in the same planar geometry as the photoelectric measurements. A round spectroscopic cuvette of 0.1 mm thickness was excited under 0° from the normal with the same light pipe as used for the photoelectric measurements. Fluorescence emission was measured under 30° from the normal. The continuous excitation light for the fluorescence induction and the preillumination came from a modified slide projector equipped with a photographic shutter. A wide band interference filter (WB 550, Ditric Optics) restricted the wavelength region of the exciting light to 530–570 nm. Fluorescence was measured for wavelengths > 665 nm (edge filter, RG 665) using a large area photodiode (OSD 300).

Theory

The mechanism of DNB quenching

The fundamental condition in the work of Sonneveld et al. [24] in distinguishing the matrix model and the model of separate units was the proof of a small average number of 'active' DNB molecules in a photosynthetic unit. It was argued that out of the large number of DNB molecules which might be dissolved in a unit, only a small fraction forming a collision complex with chlorophyll quenches the excited state efficiently ('active' DNB molecules, Chl · DNB). Since the authors did not succeed in measuring the partition coefficient of

DNB, they defined implicitly a partition coefficient which relates the dissolved DNB with the 'active' complexes in the membrane. This partition coefficient was argued to be 2 by assuming the same high quenching rate constant for the collision complex as for the trap, i.e., $k_d = 4 \cdot 10^{11}$ s^{-1}. Then, at half quenching concentration, the number of 'active' DNB-complexes is comparable to the trap number, i.e., small.

We reach the same conclusion, but by different arguments. These are based on the measured partition coefficient of DNB and the assumption of an equilibrium between separated chlorophyll and DNB molecules, and collision complexes [27]. The DNB molecules at large distance to chlorophyll shall have no quenching power. Hence, we assume an equilibrium for complex formation

$$\mathrm{Chl} + \mathrm{DNB} \underset{k_2}{\overset{k_1}{\rightleftarrows}} \mathrm{Chl \cdot DNB}$$

If all chlorophylls are equivalent, the concentration of the active complex in the membrane calculates, according to $[\mathrm{Chl \cdot DNB}]_m = K \cdot [\mathrm{Chl}]_m \cdot [\mathrm{DNB}]_m$, where $K = k_1/k_2$ and the subscript denotes concentrations in the membrane.

For the following discussion it is useful to relate the average number of collision complexes per photosynthetic unit, D, with the total DNB concentration, [Q]. The photosynthetic unit will consist of one RC plus its antenna. For convenience, we have defined a partition coefficient, Γ, according to

$$\Gamma = [\mathrm{DNB}]_m/[\mathrm{Q}] \tag{1}$$

(This definition of a partition coefficient deviates from the usual one, which is defined as $[\mathrm{DNB}]_m/c_s$ where c_s is the DNB concentration in the water phase.) Considering that the antenna size, N_o of a given photosynthetic unit is defined as the ratio of the chlorophyll concentration, $[\mathrm{Chl}]_m$, and the RC concentration, $[\mathrm{RC}]_m$, $N_o = [\mathrm{Chl}]_m/[\mathrm{RC}]_m$ belonging to that unit, and that $[\mathrm{DNB}]_m = \Gamma[\mathrm{Q}]$, the number of active DNB molecules in a unit is:

$$D = K\Gamma N_o[\mathrm{Q}] \tag{2}$$

It is this equation that yields the second abscissa in Fig. 4b.

Theory of DNB quenching without distinction between α- and β-centers

We first consider the matrix model in which statistical effects are smeared out due to the large number of photosynthetic units visited by an exciton before it becomes trapped.

For a system of equal photosynthetic units with open traps, the fluorescence quantum yield is given by:

$$\Phi_{F_o} = \frac{k_f}{k_1 + k_t + k_q K \Gamma N_o[\mathrm{Q}]} \tag{3}$$

where k_f is the statistical average rate constant of fluorescence, k_1 the statistical average rate constant of all loss processes except artificial quenching but including fluorescence, and k_t is the statistical average rate constant of trapping. (Note that these rate constants refer to one photosynthetic unit and are defined differently from those by Sonneveld et al. [24], who use rate constants referring to an excited chlorophyll molecule.) k_q is the rate constant for chlorophyll quenching by the artificial quencher. Notice that the product term to the right of k_q equals the average number of DNB molecules per photosynthetic unit, D, as defined by Eqn. 2.

In the case of closed traps, the fluorescence quantum yield is different. This may be accounted for by a different quenching efficiency of the trap, k_t':

$$\Phi_{F_{max}} = \frac{k_f}{k_1 + k_t' + k_q K \Gamma N_o[\mathrm{Q}]} \tag{4}$$

Finally, the quantum yield of trapping (all traps open), Φ_t, reads:

$$\Phi_t = \frac{k_t}{k_1 + k_t + k_q K \Gamma N_o[\mathrm{Q}]} \tag{5}$$

For convenience the expressions for the yields (Eqns. 3–5) will be normalized to the yields without a quencher ([Q] = 0) and written in the usual reciprocal way after Stern-Volmer (Stern-Volmer plots). The reciprocal normalized yields are:

$$\Phi_{F_o,N}^{-1} = 1 + \frac{k_q K \Gamma N_o}{k_1 + k_t}[\mathrm{Q}] = 1 + m_{F_o}[\mathrm{Q}] \tag{6}$$

$$\Phi_{F_{max},N}^{-1} = 1 + \frac{k_q K \Gamma N_o}{k_1 + k_t'}[Q] = 1 + m_{F_{max}}[Q] \quad (7)$$

$$\Phi_{t,N}^{-1} = 1 + \frac{k_q K \Gamma N_o}{k_1 + k_t}[Q] = 1 + m_t[Q] \quad (8)$$

where m_{F_o}, $m_{F_{max}}$, and m_t are the slopes of the resulting straight lines.

Note that the right-hand sides of Eqns. 6 and 8 are identical. This is a direct consequence of the assumption of the presence of one homogeneous antenna system with competitive decay processes. If in experiments which measure the slopes m_{F_o} and m_t by independent methods, different slopes are found, it must be concluded that the assumption of a single uniform photosynthetic unit is not valid. This argument, among others, has been used in Ref. 29 to show that the fluorescence at F_o and the light-gradient photovoltage originate from different photosystems.

We consider next the presence of two photosystems with different rate constants. Hence, Eqns. 6–8 would have to be duplicated by indexing them with 'PS I' and 'PS II'. However, from the simplifying assumption that all fluorescence is due to PS II (see Discussion), it follows that there are no equations for PS I corresponding to Eqns. 6 and 7. Then, only one additional equation (corresponding to Eqn. 8) is needed to describe the trapping efficiency of PS I:

$$\Phi_{t,N}^{-1}(\text{PS I}) = 1 + \frac{K \Gamma k_q N_o^{\text{PS I}}}{k_1 + k_t^{\text{PS I}}}[Q] = 1 + m_t^{\text{PS I}}[Q] \quad (9)$$

This equation implies the following plausible assumptions: (i) the rate constant for quenching by the artificial quencher; (ii) the rate constants of the loss processes; and (iii) the partition coefficients, Γ, are the same for PS I and PS II (see Discussion).

If one makes the further simplifying assumption that PS I and PS II have the same antenna size, then one obtains simple relations between the slopes (m_{F_o}, $m_{F_{max}}$, $m_t^{\text{PS I}}$) and the rate constants:

$$\frac{m_t^{\text{PS I}}}{m_{F_{max}}} = \frac{k_1 + k_t'}{k_1 + k_t^{\text{PS I}}} \approx \frac{k_1 + k_t'}{k_t^{\text{PS I}}} \quad (10)$$

$$\frac{m_t^{\text{PS II}}}{m_{F_{max}}} = \frac{k_1 + k_t'}{k_1 + k_t^{\text{PS II}}} \approx \frac{k_1 + k_t'}{k_t^{\text{PS II}}} \quad (11)$$

The approximation is valid when the photosynthetic quantum yield is near 1. This is equivalent to the condition $k_t \gg k_1$.

To find the correlation between the relative yields measured here and the fluorescence decay kinetics reported in the literature, we solve the differential equation for the fate of the singlet excited state, I^*, under F_{max} conditions (no artificial quencher present):

$$\frac{dI^*}{dt} = -I_o^* k_1 - I_o^* k_t' \quad (12)$$

$$I^*(t) = I_o^* e^{-(k_1 + k_t')t} = I_o^* e^{-t/\tau_{F_{max}}} \quad (13)$$

where $\tau_{F_{max}} = 1/(k_1 + k_t')$. Hence, numerical values for the term $(k_1 + k_t')$ appearing in Eqns. 10 and 11 can be taken from fluorescence decay measurements.

If we finally convert the rate constants into exponential time constants ($k = 1/\tau$), then Eqns. 10 and 11 adopt the simple form

$$\frac{m_t^{\text{PS I}}}{m_{F_{max}}} = \frac{\tau_t^{\text{PS I}}}{\tau_{F_{max}}} \quad (10a)$$

$$\frac{m_t^{\text{PS II}}}{m_{F_{max}}} = \frac{\tau_t^{\text{PS II}}}{\tau_{F_{max}}} \quad (11a)$$

where $\tau_t^{\text{PS I}}$ and $\tau_t^{\text{PS II}}$ represent the usual average trapping times of PS I and PS II, respectively.

Theory of DNB quenching with consideration of α- and β-centers

In this section we give starting equations for the quenching of DNB, when the fluorescence originates from two different units, for instance, PS II_α and PS II_β. Here, both units shall be assumed to be organized according to the matrix model. The case of matrix units plus separate units is considered later. The relative contribution of α-centers to the fluorescence yield shall be A and that of β-centers $(1 - A)$, with $0 \leqslant A \leqslant 1$. Note, that A is not the stoichiometric ratio of α- and β-centers. With open traps, the fluorescence yield in the absence of an artificial quencher is given by

$$\Phi_{F_o}(0) = A\Phi_{F_{o,\alpha}} + (1-A)\Phi_{F_{o,\beta}} = \frac{Ak_f}{k_1 + k_{t,\alpha}} + \frac{(1-A)k_f}{k_1 + k_{t,\beta}} \quad (14)$$

where the indices α and β refer to the α- and

β-centers. To obtain the expression for the fluorescence yield at F_{max}, the rate constants, $k_{t,\alpha}$ and $k_{t,\beta}$, in Eqn. 14 have to be substituted for $k'_{t,\alpha}$ and $k'_{t,\beta}$. In addition, one has to consider that the relative fluorescence yield, A, may be different for F_o and F_{max}.

In the presence of an artificial quencher, different antenna sizes of α- and β-centers may become a factor. If the antenna size of α-centers is N_o and that of β-centers, M_o, the fluorescence yield at F_o, for exmple, reads:

$$\Phi_{F_o}(Q) = \frac{Ak_f}{k_1 + k_{t,\alpha} + k_q K \Gamma N_o [Q]} + \frac{(1-A)k_f}{k_1 + k_{t,\beta} + k_q K \Gamma M_o [Q]} \quad (15)$$

The equation implies that (i) the rate constant for quenching by the artificial quencher, (ii) the rate constants of the loss processes, and (iii) the partition coefficient, Γ, are the same for PS II_α and PS II_β.

The expression for the reciprocal normalized yield follows directly from Eqn. 15:

$$\Phi^{-1}_{F_o,N}(Q, \alpha, \beta) = \frac{\Phi_{F_o}(0)}{\Phi_{F_o}(Q)} \quad (16)$$

Corresponding equations for the fluorescence yield at F_{max} can simply be obtained by the substitution mentioned before.

In the general case, Eqn. 16 no longer gives a straight line. An example is illustrated in Fig. 1, which presents a set of curves calculated for different ratios of α- and β-centers by changing only the parameter A and fixing the other parameters. It is clearly seen that only pure populations of α- and β-centers give straight lines in the Stern-Volmer plots, whereas mixed populations display negative curvatures.

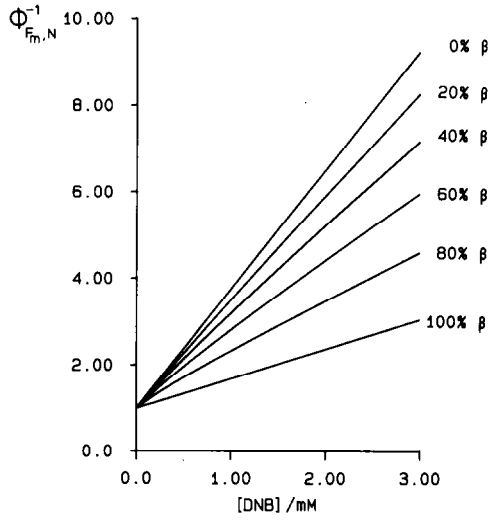

Fig. 1. The reciprocal normalized fluorescence yields arising from two different photosystems (PS II_α and PS II_β) as a function of the DNB concentration, according to Eqns. 15 and 16. The parameter was the stoichiometric ratio of the photosystems (right column). To demonstrate a pronounced curvature we chose $M_o = N_o$. The other parameters are: $k_q K \Gamma N_o = 1.1 \cdot 10^{12}\ s^{-1}$, $(k_1 + k'_{t,\alpha})^{-1} = 2.5$ ns and $(k_1 + k'_{t,\beta})^{-1} = 620$ ps.

Theory of DNB quenching for separate units

If only few quenching complexes in a unit are responsible for the quenching effect and if no excitation energy exchange takes place between different units, it is necessary to consider units with 0, 1, 2,... quenching complexes. The probability of a unit's containing i quencher molecules is given by Poisson's formula:

$$P_i = \frac{e^{-D} \cdot D^i}{i!} \quad (17)$$

where D is given by Eqn. 1 and the trapping yield for open traps in a separate unit model reads:

$$\Phi_t = \sum_i P_i \cdot \left(\frac{k_t}{k_1 + k_t + k_q \cdot i} \right) \quad (18)$$

It is trivial to derive the analogous equations for F_o and F_{max}.

The Stern-Volmer plots of Eqn. 18 and analogous ones always display a positive curvature. Therefore, it is conceivable that a negative curvature due to the α,β-heterogeneity and a positive curvature due to the separate units may, in principle, cancel each other. This weakens the argument of Sonneveld et al. [24] in favor of a matrix organization of the PS II antenna based on the observed straight lines for F_o and F_{max}, since the α,β-heterogeneity has not been included in their theory.

Results

Partition coefficient of DNB

The partition coefficient, Γ, of DNB between water and thylakoid membranes was determined by measuring the DNB concentration in the supernatant after centrifugation of the chloroplasts and measuring the membrane volume gravimetrically. The membrane volume was also estimated from literature data.

The amount of DNB dissolved in the membranes was determined at a total DNB concentration of [Q] = 1 mM in 1 ml chloroplast suspension (chlorophyll concentration of 3.5 mM). After pelletting the chloroplasts by centrifugation (5000 × g), the DNB concentration in the supernatant, c_s, was measured spectrophotometrically ($\epsilon_{235\,nm} = 1.5 \cdot 10^4\ M^{-1} \cdot cm^{-1}$). The reference cuvette contained the supernatant from a parallel experiment carried out in much the same way, but omitting

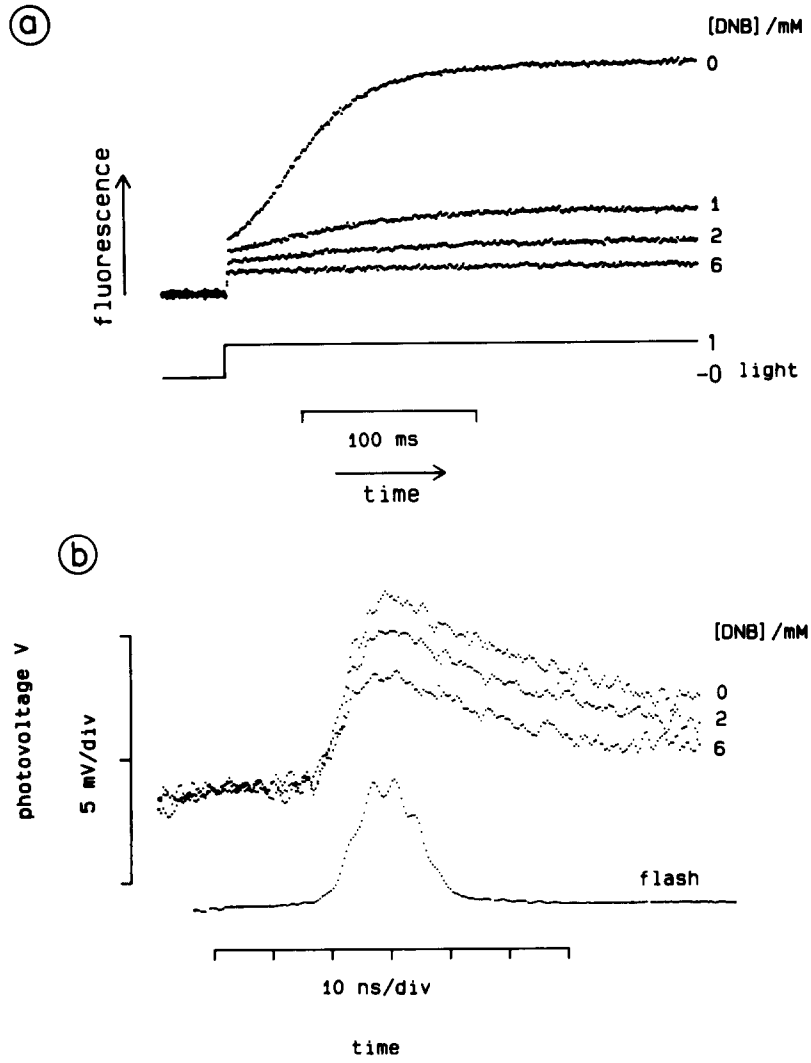

Fig. 2. (a) Examples of the effect of various concentrations of the quencher DNB on fluorescence induction curves from pea chloroplasts in the presence of 100 μM DCMU. (b) Light-gradient photovoltage from pea chloroplasts in the absence of DCMU at various concentrations of DNB (upper curves). The time-course of the exciting flash of 30 $\mu J/cm^2$ is shown in the lower curve. Averages of 20 traces.

DNB. c_s was found to be $c_s = 0.70 \pm 0.07$ mM.

To determine the membrane volume by the gravimetric method, we washed out the salts by suspending the pellet in distilled water and sedimented the membranes again. After repeating this step, the sample was dried for 1 h at 70 °C. The weight of the remaining lipid and proteins was 28 ± 2 μg. The density of the membranes was estimated by centrifugation of BBY particles through a discontinuous sucrose gradient to be 1.20 to 1.25 g/cm^3. Taking a specific weight of 1.23 g/cm^3, a membrane volume of 23 ± 2 μl is calculated for our standard conditions. From this volume and the spectroscopically determined c_s, a DNB concentration in the thylakoid membranes of $[DNB]_m = 13 \pm 2$ mM was calculated. Hence, the partition coefficient is $\Gamma = 13 \pm 2$ at our standard chlorophyll concentration of 3.5 mM.

The volume of thylakoid membranes was also estimated from the area one chlorophyl molecule occupies in the membrane, which is quoted to be 2.2 nm^2 in Refs. 30 and 31. Assuming the membrane thickness to be 5 nm, a membrane volume of 23 μl calculates for our standard conditions (1 ml; [Chl] = 3.5 mM). This volume yields also a partition coefficient for DNB of $\Gamma = 13$. In the study by Sonneveld et al. a partition coefficient of 2.5 was assumed [24].

Fluorescence quenching

The quenching effect of DNB on typical fluorescence induction curves from stacked pea chloroplasts in the presence of DCMU is illustrated in Fig. 2a. The inhibitor was added in the dark and the photoshutter was opened after a 20 min dark-adaptation period. The dependence of F_o on the DNB concentration was also measured in the absence of DCMU (curves not shown). Variations in the F_o level by measuring without or with DCMU fell within the noise level and other experimental errors. We found ratios of $F_{max}/F_0 = 4.4$–4.8 for different chloroplast preparations.

In Fig. 3a the dependences of the reciprocal fluorescence yields (normalized to the respective yields without the artificial quencher) on the DNB concentration are plotted. The data of F_{max} and F_o were subjected to a linear regression routine. The corresponding slopes are $m_{F_{max}} = 1.57$ mM^{-1} and $m_{F_o} = 0.30$ mM^{-1}. There might be a small systematic deviation (in form of a negative curvature) of the data of F_o. However, the deviation is within the experimental error.

Photovoltage quenching

The quenching effect of DNB on typical light-gradient photovoltage signals from stacked pea chloroplasts in the absence of DCMU is shown in

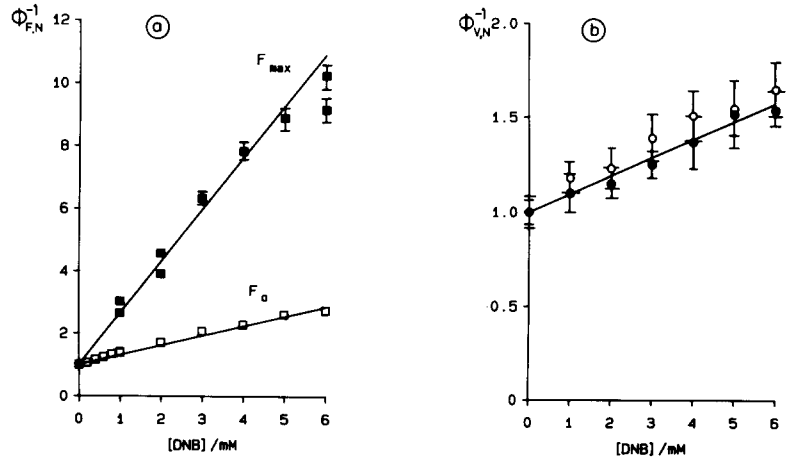

Fig. 3. (a) Stern-Volmer plots of F_o and F_{max}. The solid straight lines result from a simultaneous fit by the parameter $k_q K \Gamma N_o$ assuming the matrix model. (b) Stern-Volmer plot of the photovoltage according to the simultaneous fit. The photovoltage was measured in the absence (○) and presence (●) of 100 μM DCMU (preillumination). The correlation coefficients of the three linear regressions were within $r = 0.990 \pm 0.002$.

Fig. 2b. The rising kinetics is given by the flash duration (lower trace), whereas the decay is given by an R · C decay of the measuring cell [32,33]. At the chosen excitation energy of 30 $\mu J/cm^2$ the photovoltage amplitude responds in a linear way to the number of photosynthetic charge separations [21]. For further data analysis, readings of the peak photovoltage were made.

In Fig. 3b, the dependences of the reciprocal peak photovoltage (normalized to the respective yields without the artificial quencher) on the DNB concentration are plotted. The limited solubility of DNB does not permit concentrations higher than 6 mM. The figure included two sets of experiments. In one DCMU was present and in the other it was omitted. Taking into account all data from the two sets, the slope of the linear regression is $m_V = 0.102\ mM^{-1}$. When the data for +DCMU (closed circles) and −DCMU (open circles) are subjected separately to the linear regression routine, slightly different slopes were obtained, $m_V(-DCMU) = 0.106\ mM^{-1}$ and $m_V(+DCMU) = 0.096\ mM^{-1}$. However, the difference is near other experimental errors (small fluctuations of the laser energy or slight variations of the 100 μm spacing of the electrodes between different fillings).

Discussion

Trapping times derived from the slopes of the Stern-Volmer plots

The trapping time of PS I can be calculated from the mean fluorescence decay time at F_{max}, $\tau_{max} = 1.5$ ns, obtained from the literature, and the ratio of the slopes m_V and $m_{F_{max}}$ obtained from the present data. Since it has been shown that the photovoltage originates only from PS I [29], one can equate $m_V = m_t^{PS\,I}$. The trapping time follows from Eqn. 10a

$$\tau_t^{PS\,I} = \tau_{F_{max}} \cdot \frac{m_V}{m_{F_{max}}} = 97 \pm 10\ ps$$

This value is in good agreement with the value found by the four-component analysis of fluorescence decay [7] (Table I) and by the analysis of the rising kinetics of the PS I photovoltage [21].

The average trapping time of PS II, without considering the heterogeneity of α- and β-centers, can be calculated in the same way from the mean fluorescence decay time at F_{max} and the ratio of the slopes $m_{F_{max}}$ and m_{F_o} according to Eqn. 11a:

$$\tau_t^{PS\,II} = \tau_{F_{max}} \cdot \frac{m_{F_o}}{m_{F_{max}}} \approx 287 \pm 30\ ps$$

The such calculated average PS II trapping time is within the range obtained by three- and four-component analysis of fluorescence decay [15].

Simultaneous fit without α-, β-heterogeneity

We next want to fit simultaneously the three sets of our quenching data with one parameter, $k_q K \Gamma N_o$, under the assumption that PS I and PS II have the same antenna size and that PS II is homogeneous. PS I and PS II shall be described by a matrix model. Accordingly, Eqns. 6, 7 and 9 are valid.

Taking the fluorescence decay time at F_{max},

TABLE I

FLUORESCENCE RATE CONSTANTS AND YIELDS

Rate constants (time constants in brackets) and yields of fluorescence under F_{max} and F_o conditions taken from the four-component decay analysis in Ref. [7]. The yields were calculated by multiplying the area under the spectral curves with the respective time constant.

	F_{max}		F_o	
	rate constant $(k_1 + k_t)\ (s^{-1})$	yield (%)	rate constant $(k_1 + k_t)\ (s^{-1})$	yield (%)
PS II_α	$5.4 \cdot 10^8$ (1.9 ns)	76	$3.7 \cdot 10^9$ (270 ps)	50
PS II_β	$1.6 \cdot 10^9$ (620 ps)	19	$1.9 \cdot 10^9$ (530 ps)	32
PS I	$1.0 \cdot 10^{10}$ (100 ps)	6	$1.2 \cdot 10^{10}$ (85 ps)	18

$(k_1 + k_t')^{-1} = 1.50$ ns, the corresponding quenching line in Fig. 3a is fit by $k_q K \Gamma N_o = 1.10 \cdot 10^{12}$ s^{-1}. If we insert this value into Eqn. 9 we obtain for $(k_1 + k_t^{PS\,I})^{-1} = 100$ ps and for $(k_1 + k_t^{PS\,II})^{-1} = 285$ ps. As can be expected, these latter two values lie reasonably close to the ones determined in the previous paragraph. However, the essence of this fit is to obtain a numerical value for the product $k_q K \Gamma N_o$.

Simultaneous fit with α-, β-heterogeneity

It is obvious that the present quenching data alone do not allow for a separation of α- and β-centers. However, our quenching data shall now be used as a test for the four-component analysis of fluorescence reported by Schatz and Holzwarth [7]. This will give a more confident determination of the parameter $k_q K \Gamma N_o$. We attempt to fit simultaneously the three sets of our data by the parameters $k_q K \Gamma N_o$, $A(F_{max})$ and $A(F_o)$ under the assumption that PS II_α, PS II_β and PS I are described by a matrix model. A further fit parameter was the relative antenna size of β-centers, $M_o = f \cdot N_o$.

Stern-Volmer plots for different values of A are shown in Fig. 4a (solid lines) together with the experimental data. Good fits by Eqns. 15 and 16 and analogous ones that lie within the experimental error could be obtained with:

$k_q K \Gamma N_o = (1.10 \pm 0.02) \cdot 10^{12}$ s^{-1}

$f = 0.55 \pm 0.03$

$A(F_{max}) = 0.80 \pm 0.06$

$A(F_o) = 0\text{–}1$

The condition that the term $k_q K \Gamma N_o$ and f shall be the same for F_{max}, F_o and V turned out to be a convergence criterion for just these two parameters. The relative fluorescence yield at F_{max} agrees with the ones given by Schatz and Holzwarth in Ref. 7. The extremely wide range of $A(F_o)$ that fits our data is due to the particular combination of relative rate constants and antenna sizes valid for pea chloroplasts. In contrast to F_{max}, there is hardly any dependence of the slope of F_o on A.

An extended analysis of our fluorescence data that takes into account the contribution of PS I to the total fluorescence (data taken from Ref. 7) did not display marked differences.

The quenching rate constant and the antenna size

The equilibrium constant, K, can be estimated from the complex formation between bacteriopheophytin and DNB reported in Ref. 27. From the ratio of the association and dissociation rate con-

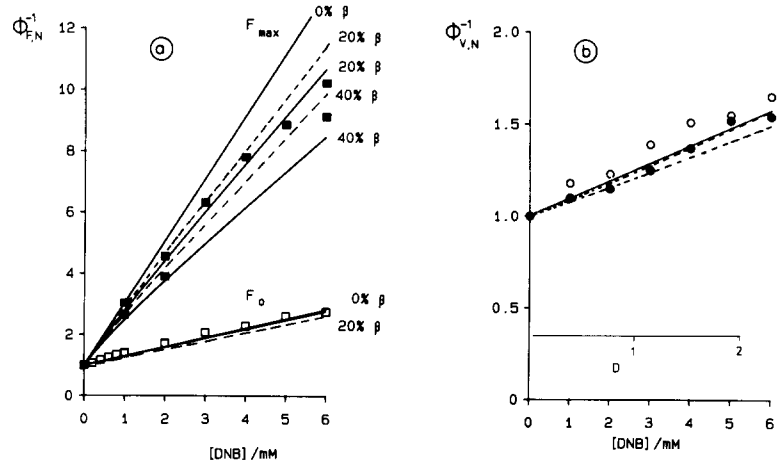

Fig. 4. (a) Stern-Volmer plots of F_{max} and F_o, taking into account α- and β-heterogeneity. Solid lines: matrix model for α- and β-centers. Dashed lines: matrix model for α-centers and separate units model for β-centers. For the derivation of the fit parameters see text. Contribution of β-centers to the fluorescence yield $(1 - A)$ as indicated. (b) Stern-Volmer plots of the photovoltage according to the simultaneous fit (matrix model, solid straight line) and fits with a separate unit model according to Eqns. 17 and 18 (dashed curved lines). The fit parameters for the separate unit case are: $K = 0.113$, $\Gamma = 13$, $N_o = 280$ and $k_q = 2.75 \cdot 10^9$ s^{-1} (lower dashed curve) or $k_q = 3.14 \cdot 10^9$ s^{-1}, respectively (upper dashed curve).

stants quoted in this reference, $K = 0.113\ M^{-1}$ follows. Assuming that this equilibrium constant is also valid in thylakoid membranes, and from our measured partition coefficient, $\Gamma = 13$, we calculate for the product

$$k_q \cdot N_o = 7.5 \cdot 10^{11}\ s^{-1}$$

and note that this number is indefinite by the unknown actual equilibrium constant K that was not determined by us. The product $k_q \cdot N_o$ corresponds to the quenching rate constant, k_d, in Sonneveld's work, who assumed $k_d = 4 \cdot 10^{11}\ s^{-1}$ [24]. Holten et al. [27] give an estimate of $k_d > 10^{11}\ s^{-1}$.

The quenching rate constant of $k_d \approx 7.5 \cdot 10^{11}\ s^{-1}$ found by us is 2–3-times larger than the rate constant for the photochemical charge separation in the RC of PS I [34]. The difference may be interpreted by the assumption that the excitation energy is deactivated when it visits a Chl · DNB complex for the first time, whereas it is converted by the photochemical trap of PS I after the second to third visit. This interpretation agrees remarkably well with the conclusions of Owens et al. [34].

In independent experiments we have measured the antenna size of PS I of our pea chloroplasts to be $N_o = 280$ (unpublished data). This allows to calculate the quenching rate constant for DNB in a photosynthetic unit to be $k_q = 2.7 \cdot 10^9\ s^{-1}$.

Fit of the PS I photovoltage with a separate unit model

With the quenching rate constant determined in this way, it is now possible to calculate a fit to the photovoltage data with the equations derived for the separate unit model. Using Eqn. 1, 17 and 18 we obtain the dashed curve in Fig. 4b.

It is obvious that the PS I data are as well described by a separate unit model as by a matrix model. The positive curvature is too small to exceed the experimental error. Therefore, no distinction is possible between the two extreme models of antenna organization.

We also tried to fit the F_o data with a separate unit model for β-centers and a lake model for α-centers (Fig. 4a, dashed lines). In this case we did not find common values for $k_q K \Gamma N_o$ and A terms that fitted our data and gave fluorescence yields lying in the range given in Ref. 7 (Table I). However, a 20% difference in the term $k_q K \Gamma N_o$ for α- and β-centers sufficed for a good fit.

Conclusions

The application of the artificial fluorescence quencher DNB upon pea chloroplasts has revealed the following results:

(1) The existence of α- and β-centers may result in a negative curvature of the Stern-Volmer plots as predicted by Eqn. 15. This curvature is opposed to the positive curvature predicted for separate unit models. Since the curvatures might cancel each other so as to yield an apparent straight line, the experimental observation of straight lines by Sonneveld et al. [24] and ourselves cannot be taken as a stringent criterion to distinguish different organizations of antenna systems.

(2) The mean trapping time in PS I was deduced to be 97 ± 10 ps by measuring the quenching effect on a non-time resolved photovoltage and using the time constant of the fluorescence decay at F_{max}.

(3) Similarly the mean average trapping time in PS II has been determined to be 285 ps by measuring the quenching effect on F_o and using the time constant of the fluorescence decay at F_{max}.

(4) A chlorophyll-DNB complex is a more efficient trap than the reaction center of PS I.

Acknowledgements

The authors thank Prof. W. Junge for helpful discussions and continous support of this work. The financial support of the Deutsche Forschungsgemeinschaft (SFB 171) is acknowledged.

References

1 Thorne, S.W. and Duniec, J.T. (1983) Q. Rev. Biophys. 16, 197–278.
2 Van Grondelle, R. (1985) Biochim. Biophys. Acta 811, 147–195.
3 Geacintov, N.E. and Breton, J. (1987) Crit. Rev. Plant Sci. 5, 1–44.
4 Boardman, N.K., Thorne, S.W. and Anderson, S.W. (1966) Proc. Natl. Acad. Sci. USA 56, 586–593.
5 Holzwarth, A.R., Wendler, J. and Haehnel, W. (1985) Biochim. Biophys. Acta 807, 155–167.

6 Wendler, J. and Holzwarth, A.R. (1988) Biophys. J., in press.
7 Schatz, G.H. and Holzwarth, A.R. (1987) Progress in Photosynthesis Research (Biggins, J., ed.), Vol. I, pp. 67–69, Martinus Nijhoff, Dordrecht.
8 Joliot, A. and Joliot, P. (1964) C.R. Acad. Sci. Paris Ser. D. 278, 4622–4625.
9 Melis, A. and Homann, P.H. (1975) Photochem. Photobiol. 21, 431–437.
10 Melis, A. and Homann, P.H. (1976) Photochem. Photobiol. 23, 343–350.
11 Melis, A. and Homann, P.H. (1978) Arch. Biochem. Biophys. 190, 523–530.
12 Hodges, M. and Moya, I. (1986) Biochim. Biophys. Acta 849, 193–202.
13 Melis, A. and Duysens, L.N.M. (1979) Photochem. Photobiol. 29, 373–382.
14 Thielen, A.P.G.M. and Van Gorkom, H.J. (1981) Biochim. Biophys. Acta 635, 111–120.
15 Holzwarth, A.R. (1986) Photochem. Photobiol. 43, 707–725.
16 Magde, D., Berens, S.J. and Butler, W.L. (1982) Proc. Soc. Photo. Opt. Instrum. Eng. 322, 80–86.
17 Gulotty, R.J., Fleming, G.R. and Alberte, R.S. (1982) Biochim. Biophys. Acta 682, 322–331.
18 Witt, H.T. and Zickler, A. (1973) FEBS Lett. 37, 307–310.
19 Fowler, C.F. and Kok, B. (1974) Biochim. Biophys. Acta 357, 308–310.
20 Trissl, H.-W. and Kunze, U. (1985) Biochim. Biophys. Acta 806, 136–144.
21 Trissl, H.-W., Leibl, W., Deprez, J., Dobek, A. and Breton, J. (1987) Biochim. Biophys. Acta 893, 320–332.
22 Vredenberg, W.J. and Duysens, L.N.M. (1963) Nature 197, 355–357.
23 Etienne, A.L., Lemasson, C. and Lavorel, J. (1974) Biochim. Biophys. Acta 33, 288–300.
24 Sonneveld, A., Rademaker, H. and Duysens, L.N.M. (1980) Biochim. Biophys. Acta 593, 272–289.
25 Delepelaire, P. and Bennoun, P. (1978) Biochim. Biophys. Acta 502, 183–187.
26 Breton, J. and Geacintov, N.E. (1980) Biochim. Biophys. Acta 594, 1–32.
27 Holton, D., Windsor, M.W., Parson, W.W. and Gouterman, M. (1978) Photochem. Photobiol. 28, 951–961.
28 Polle, A. and Junge, W. (1986) Biochim. Biophys. Acta 848, 257–264.
29 Trissl, H.-W., Breton, J., Deprez, J. and Leibl, W. (1987) Biochim. Biophys. Acta 893, 305–319.
30 Wolken, J.J. and Schwertz, F.A. (1953) J. Gen. Physiol. 37, 111–120.
31 Thomas, J.B., Minnaert, K. and Elbers, P.D. (1956) Acta Bot. Neerl. 5, 314–321.
32 Trissl, H.-W. (1985) Biochim. Biophys. Acta 806, 124–135.
33 Trissl, H.-W. and Kunze, U. (1985) Biochim. Biophys. Acta 806, 136–144.
34 Owens, T.G., Webb, S.P., Metz, L., Alberte, R.S. and Fleming, G.R. (1987) Proc. Natl. Acad. Sci. USA 84, 1532–1536.